Efficient solvothermal synthesis of highly porous UiO-66 nanocrystals in dimethylformamide-free media

Luis A. Lozano, Clara M. Iglesias, Betina M.C. Faroldi, María A. Ulla & Juan M. Zamaro

Journal of Materials Science
Full Set - Includes `Journal of Materials Science Letters'

ISSN 0022-2461

J Mater Sci
DOI 10.1007/s10853-017-1658-5

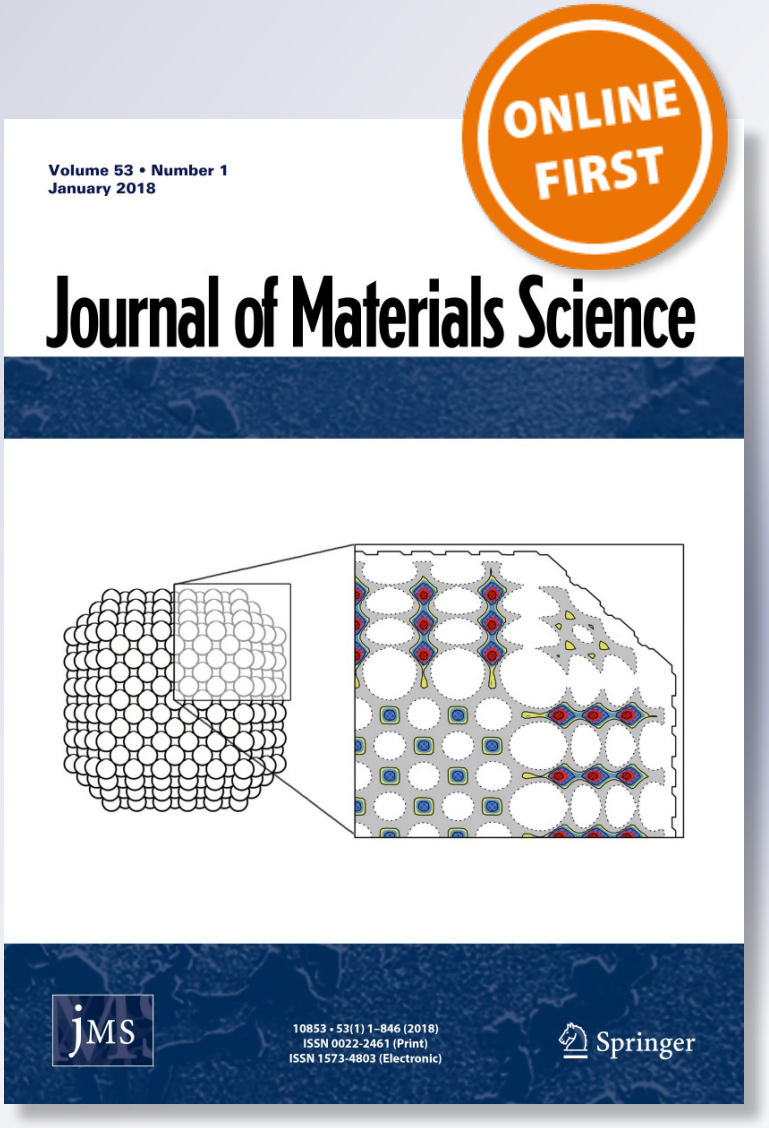

Springer

J Mater Sci

Chemical routes to materials

Efficient solvothermal synthesis of highly porous UiO-66 nanocrystals in dimethylformamide-free media

Luis A. Lozano[1], Clara M. Iglesias[1], Betina M.C. Faroldi[1], María A. Ulla[1], and Juan M. Zamaro[1,*]

[1] *Instituto de Investigaciones en Catálisis y Petroquímica, INCAPE (FIQ, UNL, CONICET), Santiago del Estero, 2829 (3000), Santa Fe, Argentina*

Received: 4 September 2017
Accepted: 5 October 2017

ABSTRACT

The UiO-66 metal–organic framework has remarkable physicochemical characteristics which have positioned it as one of the Zr-MOFs with greater potential for application in diverse processes. However, it remains a challenge how to optimize the synthesis methods so as to obtain this material with high yield and good porous properties under more eco-compatible conditions. In this work, we report the solvothermal synthesis of UiO-66 nanocrystals with high surface area using acetone as the synthesis medium, replacing the traditional and toxic *N*,*N*-dimethylformamide. The effects of solvents, reactant concentration, temperature, synthesis time and mixture protocol on the material properties were characterized by XRD, SEM–EDS, FTIR, TGA-SDTA and N_2 adsorption isotherms. The sample obtained in pure acetone employing the optimized protocol exhibited spherical nanoparticles 150 nm in size and presented the greatest relative crystallinity. The alternative protocol allowed obtaining UiO-66 with high yields (~ 91%) without employing DMF, under mild conditions (80 °C), in the form of nanocrystals with high specific surface area (1299 $m^2\ g^{-1}$) that can be activated by simple drying at 130 °C and atmospheric pressure. The MOF obtained in acetone under optimum conditions showed reversible CO_2 uptake capacity at room temperature and low pressures as determined by both CO_2 isotherms and TGA-CO_2 tests.

Introduction

The metal–organic framework (MOF) called UiO-66 is a microporous zirconium terephthalate which consists of clusters of zirconium atoms connected to each other by molecules of benzenedicarboxylates, forming a three-dimensional arrangement. This MOF was synthesized for the first time in 2008 [1] and has interesting physicochemical qualities such as high thermal, chemical and mechanical stability [1, 2] as well as high specific surface area. The material has a pore system composed of two cages with free diameters of approximately 11 and 8 Å, respectively, connected through narrow triangular windows with an opening of about 6 Å [1, 3]. These properties have

Address correspondence to E-mail: zamaro@fiq.unl.edu.ar

DOI 10.1007/s10853-017-1658-5

Published online: 12 October 2017

positioned it as one of the Zr-MOFs with greater potential for application in various processes, such as gas adsorption and storage [2–4], gas separation [5], drug release [6], sensor [7] and catalysis [8, 9], among others. In general for MOFs synthesis, other more environmentally-friendly approaches have been analyzed apart from solvothermal methods, e.g., those that use small amounts of solvent [10], solvent-free methods like mechanosynthesis [11] or methods that require lower temperature or shorter reaction times such as sonocrystallization [12], microwave-assisted synthesis [13] or synthesis by microfluidic approach [14]. However, currently most of the reported procedures for obtaining crystals of UiO-66 involve solvothermal treatments using *N*,*N*-dimethylformamide (DMF) as solvent and generally temperatures of 120 °C [1–9]. In this line, several studies have been carried out in order to obtain different Zr-MOFs; their synthetic protocols generally involve solvothermal treatments at high temperatures and pressures [15]. In the case of UiO-66, the inclusion of additives such as water [16], several acids (HCl, benzoic, acetic, trifluoroacetic, formic and hydrofluoric) [16–21] and bases (NH_4OH) [22], used to optimize the synthesis and improve the properties of the material has been analyzed, in all cases DMF being the solvent used for its obtention. In addition, the quantitative relationships between the features of these additives (called modulators) and the properties of this MOF have been proposed [23]. UiO-66 with moderate surface area (783 $m^2\ g^{-1}$) and BDC impurities was obtained solvothermally (120 °C) using ethanol [24] and also mixtures of 40–60% v/v of acetic acid–water heated under reflux (769 $m^2\ g^{-1}$) which, in addition, showed structural defects [25].

In this context, an aspect of great interest emerges, i.e., to optimize the synthetic protocol taking into account more ecological and economic criteria, such as using less toxic and expensive solvents than DMF as well as milder treatment conditions. DMF is a very toxic solvent which has not yet been classified as carcinogenic to humans but which, according to substantial evidence, causes birth defects, affects the nervous system as well as the liver and kidney [26]. In addition, due to its low vapor pressure (3.87 mm Hg at 25 °C) and kinetic diameter of about 0.55 nm [27], after the MOF synthesis certain activation steps are required, including long contact times with other volatile solvents such as chloroform [4, 22], methanol [5], or ethanol [28] to perform solvent exchanges; afterward, controlled drying in vacuum stoves is also required to obtain the permanent porosity of the material. This is a delicate operation that can cause partial blocking or collapse of the MOF channels [28] or induce intercrystalline defects [27], also contributing to the large dispersion of specific surface area values reported in the literature. On the other hand, acetone is a very common solvent which is used in numerous applications that, although is not completely innocuous, it presents a low acute and chronic toxicity both ingested and inhaled [29]. In addition, it has a high vapor pressure (231 mm Hg at 25 °C) and a kinetic diameter of 0.46 nm [30], which could help in the post-synthesis activation step.

In this work, we study the solvothermal synthesis protocol to obtain UiO-66 in more sustainable conditions, replacing the use of *N*,*N*-dimethylformamide by a reaction mixture based on acetone employing mild treatments (80 °C). The physicochemical qualities of the solids were analyzed, and the best material obtained was also evaluated in its capacity to interact with CO_2 at low pressures and room temperature as a probe test.

Experimental

Synthesis procedure

Benzenedicarboxylic acid (BDC, Aldrich), $ZrCl_4$ (Zr, Aldrich) and acetone (Cicarelli, 99.0% purity) were used without further purification. In some experiments ethanol (Cicarelli proanalysis, 99.5% purity), *N*,*N*-dimethylformamide (Aldrich) and distilled water were also used. Three different protocols of mixture of reactives were used, as indicated in the scheme of Fig. 1. The mixture procedure basically consisted in mixing the two solid reactants together with the solvent in the molar proportions BDC: $ZrCl_4$: solvent = 1:1:2433, 1:1:1622, 1:1:750 or 1:1:375. The above indicated reactants to solvent molar ratios were denoted as *R*1, *R*2, *R*3 and *R*4, respectively. After obtaining the homogeneous mixture, it was placed under solvothermal treatments between 40 and 160 °C during different times (6–72 h). At the end of the treatments, the solids were recovered by centrifugation (10000 rpm, 10 min), washed twice with ethanol and finally dried at 80 °C overnight. The samples were denoted by indicating the protocol number (1, 2 and 3), the used solvent (D: DMF, A:

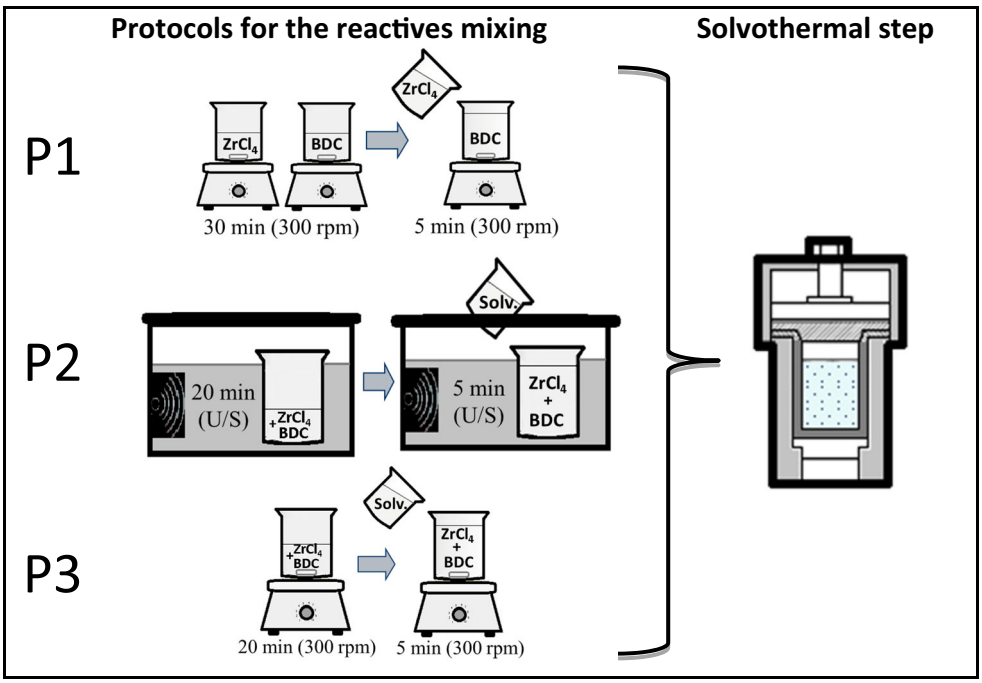

Figure 1 Scheme of the three protocols employed for the mixture of reactants before the solvothermal treatment.

acetone, E: ethanol, W: water), the solvent percentage, the synthesis time between brackets, the synthesis temperature and the solvent molar ratio (R). For example, 2-A93(72)T80-R2 denotes a sample synthesized by protocol 2 with 93% v/v of acetone at 72 h and 80 °C with a BDC: $ZrCl_4$: solvent molar ratio of 1:1:1622.

Materials characterization

The microstructure of the solids obtained was examined by scanning electron microscopy (SEM) with a benchtop instrument PhenomWorld ProX (Netherlands) operated at 15 kV. The samples were coated with a thin layer of Au in order to improve the images. Elemental microanalysis and elemental mapping were carried out by energy-dispersive X-ray spectroscopy (EDS). Fourier transformed infrared spectroscopy (FTIR) of KBr-compacted samples was performed with a Shimadzu Prestige-21 instrument equipped with a DLATGS high-sensitivity detector (400–4000 cm^{-1}, 40 scans, 2 cm^{-1} resolution). X-ray diffraction (XRD) was performed with a Shimadzu XD-D1 instrument by scanning the 2θ angle at 2° min^{-1} between 5° and 60° using CuKα radiation ($\lambda = 1.5418$ Å, 30 kV, 40 mA). Adsorption–desorption isotherms of N_2 at 77 K were acquired, after the solids were degassed (4 h, 200 °C, vacuum) and the specific surface area (BET), total pore volume, micropore volume and mesopore size distribution (BJH) were obtained. Low-pressure CO_2 adsorption isotherms at 298 K were acquired in a static equilibrium adsorption system, admitting increasing CO_2 doses after an evacuation at 200 °C for 4 h under dynamic vacuum. Dynamic CO_2 uptake experiments in a TGA equipment were also performed applying cycles of CO_2 flow (298 K, 50 cm^3 min^{-1}, 60 min) using a CO_2: He mixture (50:50 v/v) interspersed by desorption stages with sweeps in N_2, heating from 25 to 200 °C at 10 °C min^{-1} in N_2 flow (50 mL min^{-1}). To analyze the thermal stability of the crystals, thermogravimetric analysis (TGA) and single differential thermal analysis (SDTA) were conducted with a Mettler Toledo STAR^e with a TGA/SDTA851e module from 25 to 900 °C at 10 °C min^{-1} in N_2 flow (50 mL min^{-1}, STP).

Results and discussion

Synthesis of UiO-66 in solvent mixtures: acetone-DMF and ethanol-DMF

Figure 2 shows the diffraction patterns of the solid obtained using pure DMF (protocol 1) in reference conditions (120 °C and 24 h), sample 1-D100(24)T120-R2. All the indexed signals of this MOF can be observed, which correspond to a symmetrical cubic

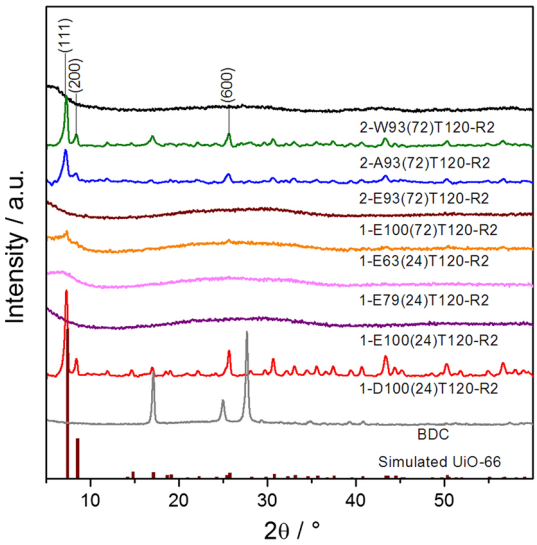

Figure 2 X-ray diffraction patterns (XRD) of the solids obtained in ethanol-DMF, acetone-DMF and water-DMF mixtures using protocol 1 with a molar ratio 1:1:1622 and at 120 °C.

structure that matches the diffractogram simulated from their crystallographic data (CCDC 733458). By replacing DMF with increasing proportions of ethanol, amorphous solids were recovered (1-E63(24)T120-R2–1-E100(24)T120-R2) even using the lowest proportion of ethanol. However, no remaining impurities, such as BDC, can be observed. The latter presented intense signals around $2\theta = 17°$ and 27° as observed in the diffractogram of the pure reagent (Fig. 2). Evidently, the only change in the synthesis medium modified the MOF formation process. In the solid obtained with a lower proportion of ethanol, 1-E63(24)T120-R2, a small signal was observed that coincides with the main peak of the MOF, which suggests an incomplete crystallization. For this reason, the treatment time was extended to 72 h, but amorphous materials were also recovered (Fig. 2). It was attempted to improve this aspect taking into account reports indicating that the addition of certain additives improves the crystallinity of this MOF obtained in DMF [15, 16]. Experiments adding small amounts of water, acetic acid, sodium acetate or pre-synthesized UiO-66 crystals were performed (not shown), but none of these variants improved crystalline qualities.

The simple mixing protocol used above (protocol 1) is analogous to that reported for the synthesis of other MOFs such as ZIF-8 and HKUST-1, but differs slightly from that originally reported by Cavka et al. [1] for UiO-66. Next, a variant of the latter (protocol 2) was used to dissolve the solids in a small amount of DMF (7% v/v) using ultrasound and then completing the final proportion with the alternative solvents (protocol 2), ethanol, acetone or water (93% v/v). This is outlined in Fig. 1. After bringing the mixtures thus prepared to solvothermal treatment with the same molar ratios and temperature as the previous series of syntheses, the recovered solids exhibited diffractograms whose main signals coincided with those of the MOF (Fig. 2) when using a mixture with ethanol (2-E93(72)T120-R2) or with acetone (2-A93(72)T120-R2), but not when using the mixture with water (2-W93(72)T120-R2). When comparing these results with those obtained using protocol 1, it is evident that the formation of the MOF is not only very sensitive to the solvent, but also to the preparation protocol of the synthesis mixture.

On the other hand, it is known that in the processes of solvothermal synthesis an increase in temperature can modify the crystallinity of the obtained materials. Therefore, starting from the previous results, 2-A93(72)T120-R2 and 2-E93(72)T120-R2, the effect of the treatment temperature was analyzed. We found that in both solvents there was an optimum temperature in which the higher crystalline development was obtained, which is 80 °C (Fig. S1). The solids synthesized under these conditions presented specific surface areas (BET) of 986 $m^2\ g^{-1}$ for 2-A93(72)T80-R2 and 864 $m^2\ g^{-1}$ for 2-E93(72)T80-R2, respectively. These results are noteworthy since pure UiO-66 phases were obtained with treatments at 80 °C, replacing the 93% v/v of DMF by acetone or ethanol.

Synthesis of UiO-66 in *N,N*-dimethylformamide-free media

When trying to completely replace DMF (employing protocol 2), it can be seen (Fig. 3) that the solid obtained in pure acetone, 2-A100(72)T80-R2, showed a low crystallinity, while that obtained in ethanol was totally amorphous (not shown). Considering the critical effect that the homogenization stage seems to have on the development of the MOF, it was reformulated using magnetic stirring (protocol 3), as shown in Fig. 1. The mixture thus obtained using ethanol, after solvothermal treatment, yielded a solid that remained as an amorphous phase (not shown), but that obtained with pure acetone and treated under the same previous conditions (72 h, 80 °C)

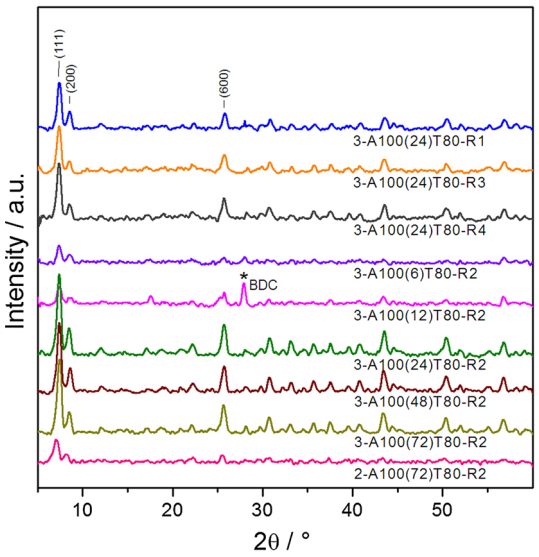

Figure 3 X-ray diffraction patterns (XRD) of the solids obtained in pure acetone at different times and molar ratios of solvent.

yielded a solid, 3-A100(72)T80-R2, which showed strong UiO-66 diffraction signals (Fig. 3). The pure UiO-66 sample thus obtained is relevant since it was possible to totally replace the DMF by acetone using mild treatment conditions. The above results also highlight a poorly discussed aspect in the literature of MOFs in general, which is the high sensitivity of the mechanism of MOF formation to both the solvent and the route of preparation of the reaction mixture. The evolution of UiO-66 phase by initially mixing the reactants together in a small amount of solvent will probably lead to the formation of the necessary precursors of hexa-Zr clusters. In addition, it is likely that our optimized protocol can be extended to other Zr-MOFs currently obtained in DMF such as the case of NU-1000 [31] and NU-1102 [32], since in their synthesis the same metal precursor $ZrCl_4$ is used, forming $Zr_6O_4(OH)_4(CO_2)_{12}$ secondary building units. However, the need for further optimizations of solvothermal treatment times and temperatures is anticipated, given the different pKa of the carboxylic acid function in the voluminous tetra carboxylated ligands of said MOFs.

Next, some critical variables were analyzed by maintaining the synthesis protocol (P3) in pure acetone discussed above, which provided a solid with a high crystalline quality. When analyzing the UiO-66 crystalline evolution with the synthesis time, it can be observed (Fig. 3) that solids with intense X-ray diffraction patterns were obtained after 48 and 24 h. However, the intensities of the main XRD signals corresponding to the (111), (200) and (600) planes indicate that the sample obtained after 24 h presented the greatest relative crystallinity and also the highest yield (Table 1). At longer times probably a slight degradation of the MOF after the prolonged contact with the synthesis medium was produced, since it also corresponded to the tendency of the solids yield. On the other hand, it is observed that after only 6 h of treatment an incipient development of a pure phase of UiO-66 occurred. In the solid obtained after 12 h, a small XRD signal of remaining BDC can be observed, which may be due to an inefficient washing of this sample.

Since it would be desirable to use as little acetone as possible and taking into account that a treatment for 24 h provided the solid with the best properties, the effect of the reagent concentration was then analyzed. The solids obtained with a smaller proportion of acetone (*R*3 and *R*4 ratios) showed developed diffractograms (Fig. 3), although their relative crystallinity was somewhat smaller compared to the medium concentration (*R*2) as shown in Table 1. Likewise, when using a greater proportion of solvent (*R*1) the quality of the MOF also decreased (Table 1), indicating that an optimum amount of acetone is required for the most efficient and crystalline formation of the UiO-66.

Physicochemical properties of UiO-66 crystals obtained in pure acetone

The FTIR spectra of synthesized materials (Fig. 4) exhibited two regions that typically characterize this MOF. An intense doublet around 1575 and 1400 cm^{-1}, corresponding to modes of stretching in and out of the plane of carboxylate groups (OCO), respectively, and a group of signals at low wavenumbers with two main peaks at 554 and 480 cm^{-1} associated with Zr–O bonds in the MOF cluster [1]. The calculated harmonic vibrational spectra assigned those signals to modes of Zr–(OC) asymmetric stretching and μ3–OH stretching (in-phase) of the (HO–Zr–OH) units, respectively [33]. When comparing the IR spectra with the XRD patterns, it can be seen that when obtaining a developed crystalline structure, on the one hand, the IR signals in the (OCO) region are narrowed and on the other hand the two low frequency signals are well defined. This effect is more noticeable when the solid has very

Table 1 Efficiency, crystallinity, textural properties and thermal stability of UiO-66 synthesized using acetone at 80 °C

Sample	Yield (%)[a]	Crystallinity (%)[b]	Specific surface area ($m^2\ g^{-1}$)[c]	Micropore volume ($cm^3\ g^{-1}$)[d]	External surface ($m^2\ g^{-1}$)[e]	Total pore volume ($cm^3\ g^{-1}$)[f]	ΔTGA1[g] (%)	ΔTGA2[h] (%)
3-A100(6)T80-R2	55.7	30	275	0.17	57	0.19	20.0	27.7
3-A100(12)T80-R2	71.9	29	421	0.17	57	0.27	21.5	26.7
3-A100(24)T80-R2	91.2	100	1299	0.52	147	0.78	34.0	24.7
3-A100(48)T80-R2	82.0	86	1158	0.46	139	0.72	29.9	27.1
3-A100(72)T80-R2	82.9	83	1036	0.44	112	0.68	33.8	25.6
3-A100(24)T80-R4	74.6	74	692	0.26	123	0.40	25.1	24.1
3-A100(24)T80-R3	69.7	58	667	0.23	94	0.59	25.7	24.0
3-A100(24)T80-R1	84.5	69	810	0.37	38	0.44	27.2	26.7

[a]Synthesis yield considering the amount of Zr added in the synthesis mixture and the amount of Zr obtained in the MOF (calculated with the theoretical formula $Zr_6O_4(OH)_4(BDC)_6$ [16])

[b]Relative crystallinity between solids, considering the sum of the integrated intensity of the main XRD signals (planes (111), (200) and (600))

[c]Calculated considering the linearization of the BET equation (using a range of $P/P_0 = 0.01–0.25$)

[d]Calculated with the t-plot method (considering $t = 0.39–0.86$)

[e]Calculated with the slope of *t*-plot graphs (St = slope × 1.5495)

[f]Calculated as the volume of the N_2 liquid adsorbed at $P/P_0 \approx 0.99$

[g]Mass loss in TGA from 25 up to 300 °C

[h]Mass loss in TGA from 425 °C to the end of the structural collapse at 600 °C

low crystalline evolution, i.e., in the sample 3-A100(6)T80-R2. The correlation between the infrared profile and the crystallinity was confirmed when analyzing several materials without crystalline development, such as the solid 1-E100(24)T120-R2 included in Fig. 4 for comparison. That is, a FTIR spectrum can qualitatively anticipate whether or not the material will exhibit good crystallinity. Our interpretation is that materials with low crystallinity correspond to zirconium terephthalates with a disordered bond connection structure in which there is a greater variation of the environment of the COO- bound to the centers of Zr. In addition, the orderly disposition of the zirconia cluster forming the $Zr_6O_4(OH)_4(BDC)_6$ units would not be fully developed, given the blurred signals at 554 and 480 cm^{-1}.

The SEM images of the solid obtained in acetone after a 6 h synthesis, 3-A100(6)T80-R2, showed spongy aggregates (Fig. 5a) without the presence of particles with a defined morphology, which is compatible with a Zr-terephthalate of low crystalline characteristics, in agreement with the previous XRD and FTIR results. Meanwhile, in the sample obtained at 12 h (Fig. 5b) clusters of nanocrystals with a size of about 300 nm forming compact aggregates can be seen. The solid obtained at 24 h, 3-A100(24)T80-R2, showed spherical nanoparticles similar to that of 12 h but with a size of about 150 nm, forming somewhat more open aggregates in the shape of clusters (Fig. 5c). This morphology differs from that found for this MOF obtained in DMF, which presents cubic inter grown single crystals [1]. The replacement of DMF by acetone not only has implications in the crystalline development of the UiO-66 phase, but also exerts marked effects on the size and morphology of the crystals, analogous to those reported for the formation of other MOFs [34, 35]. On the other hand, the solid obtained in the most dilute condition, 3-A100(24)T80-R1, presented a similar particle size and morphology than that of medium dilution, although somewhat more agglomerated (Fig. 5d). In contrast, by reducing the proportion of solvent a deep change in the crystal morphology was observed. For 3-A100(24)T80-R3 sample, in addition to nanoparticles, the material presented larger spherical formations (between 1 and 0.5 μm), some of which were fused together (Fig. 5e), while the solid synthesized with the least proportion of solvent showed a larger amount of the big spherical formations (Fig. 5f). SEM analysis indicated a strong dependence on the

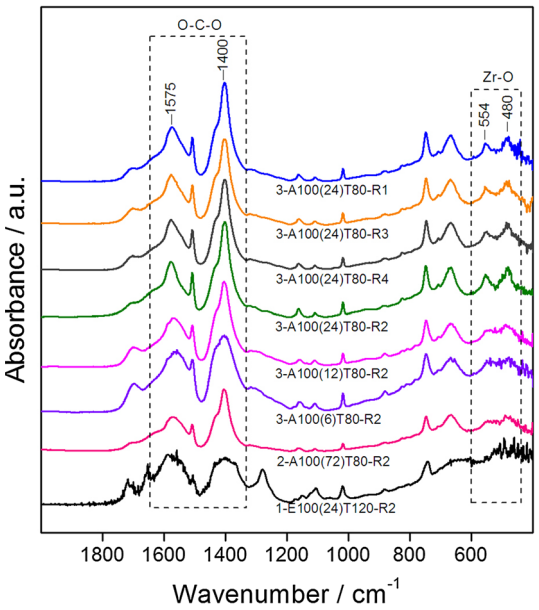

Figure 4 FTIR spectra of the samples synthesized in pure acetone under different solvothermal treatment conditions.

morphology of solids with the concentration of the reactants (at the same Zr: BDC molar ratio), especially when using concentrated conditions. To analyze the chemical characteristics of the crystals in these cases (nanoparticles and micrometer spherical particles), analyses by EDS-mapping were performed. A similar concentration and homogeneous distribution of Zr and O were observed in the sample obtained under the more concentrated conditions, 3-A100(24)T80-*R*4, both in the nano particle aggregates and in the bigger particle sectors (Fig. S2). This is compatible with a uniformly formed Zr-terephthalate and also confirms that in no sector of the solids do BDC or $ZrCl_4$ residues persist, in agreement with the XRD patterns in which only UiO-66 signals were detected. In the sample 3-A100(24)T80-R3, the situation was similar, without any differentiation in composition of the sample constituent particles. Similarly, in the 3-A100(24)T80-R2 sample, it was observed that the dispersed nanoparticles have a homogeneous composition throughout all the material (Fig S2).

The N_2 adsorption–desorption isotherms of all the solids synthesized in pure acetone (Fig. 6) correspond to Ib-type isotherms, which are found in materials having pore size distributions over a broader range including wider micropores and possibly narrow mesopores ($< \sim 2.5$ nm) [36]. The profile of this type of isotherm exhibits a less abrupt increase in the region of low pressures with a plateau with a slight inclination and has previously been seen in UiO-66 synthesized in DMF [2, 16]. In addition, the observed increase in adsorption in the region of $P/P_0 \approx 0.9$ indicates the possible presence of macropores. As the synthesis time increased, a higher adsorbed volume (Fig. 6) and a higher surface area of the solids were observed (Table 1). The sample obtained at 24 h with the ratio 1:1:1622, (3-A100(24)T80-R2) presented the highest values of surface area and micropore volume, being 1299 $m^2\ g^{-1}$ and 0.52 $cm^3\ g^{-1}$, respectively (Table 1). These values are remarkable and even higher than many others reported for this MOF obtained in reaction mixtures with DMF [Table S1]. In addition, the trend in the textural properties correlates with the efficiency of the synthesis and crystallinity of the MOF (Table 1). In the sample with better qualities, a small hysteresis was also observed (inset Fig. 6), reflecting the presence of larger mesopores, which are usually found in solids having mesoporosity due to the small size of the particles [16] which is compatible with the small crystallites that make up aggregates in this solid, as observed by SEM. The mesopore size distribution (inset Fig. 6) shows a bimodal curve with a signal at 3.7 nm and a less accentuated peak around 10 nm. On the other hand, in the other isotherms no large displacements were observed between the adsorption and desorption branches, although the values of micropore volume and total pore volume account for the presence of mesoporosity in all samples (Table 1), which is compatible with these types of isotherms. As for the solids obtained with the lowest proportion of solvent, they presented N_2 isotherms of similar characteristics although their textural properties (Table 1) were somewhat lower than those obtained with ratio 1:1:1622.

All solids obtained in pure acetone showed a high thermal stability as shown the TGA-SDTA analysis (Fig. 7). Initially, there is a mass loss that extends up to 130 °C associated with physisorbed water and host molecules, such as solvent residues trapped in the MOF pores. The magnitude of this event in the different samples followed a logical tendency with the specific surface area, respectively (Table 1). An important fact to note from TGA results is the possibility of releasing the permanent porosity of the UiO-66 by a simple drying process at atmospheric pressure at 130 °C, with the consequent economic advantage and considering that the activation is a delicate and time-consuming operation. After the first

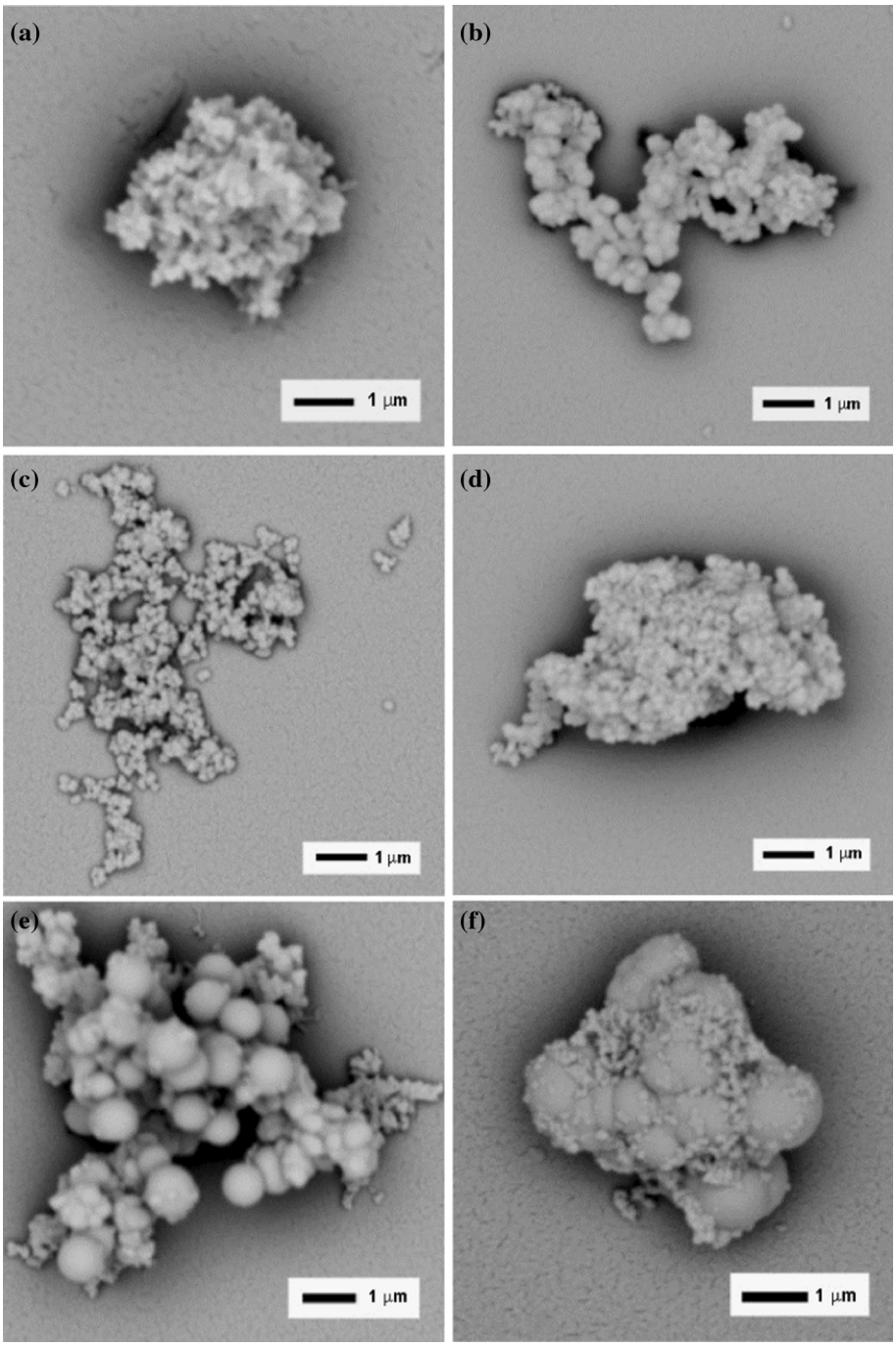

Figure 5 SEM images of the samples synthesized in pure acetone under different solvothermal treatment conditions.

step of mass loss, another small evolution starts at 200 °C, assigned to the dehydroxylation processes of the MOF cluster from $Zr_6O_4(OH)_4$ to Zr_6O_6 [1, 2, 16, 33]. Subsequently, from 425 °C, the collapse of the MOF structure begins due to the thermal degradation of the ligand. The mass loss in this region (Table 1) was in all cases significantly lower than the stoichiometric proportion, indicating missing linkers in these materials [2, 4, 33, 37]. The SDTA analysis acquired simultaneously (inset in Fig. 7), showed endothermic and exothermic evolutions at the same temperatures of the TGA events, in line with the described processes. It is important to note that even the sample with the lowest crystallinity and porosity, 3-A100(6)T80-R2, exhibited a thermal stability similar to that of the more developed crystals. This supports the claim that the robustness of the UiO-66 framework is mainly associated with the

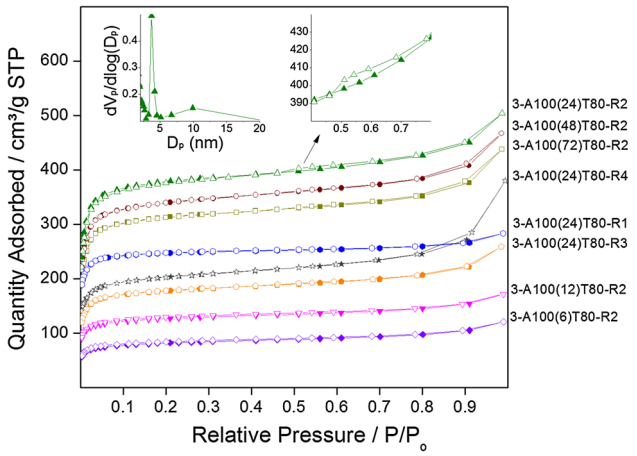

Figure 6 N_2 adsorption–desorption isotherms at 77 K of the samples synthesized in pure acetone under different solvothermal conditions. The insets of the solid obtained with 1:1:1622 molar ratio show the hysteresis in the adsorption–desorption branches (right) and the distribution of mesopores by the BJH method (left).

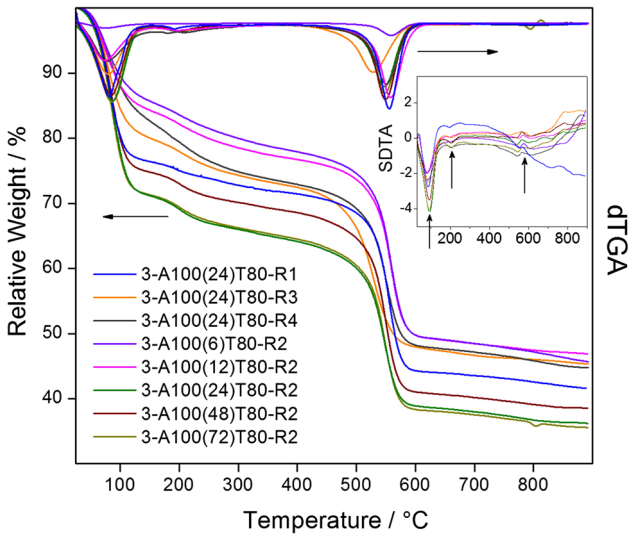

Figure 7 TGA, dTGA and SDTA analysis of the UiO-66 obtained in pure acetone under different solvothermal conditions.

strong bonds between zirconium and carboxylate (Zr-OC), rather than with the development of the ordered structure of Zr_6 clusters in the porous array of the MOF. In addition, the TGA results reinforce the interpretation of the IR spectra of the less crystalline samples, which would correspond to more amorphous terephthalates with disordered bonding environments.

The material that presented the best properties, 3-A100(24)T80-R2, was analyzed in its capacity of adsorption of CO_2 at room temperature and low

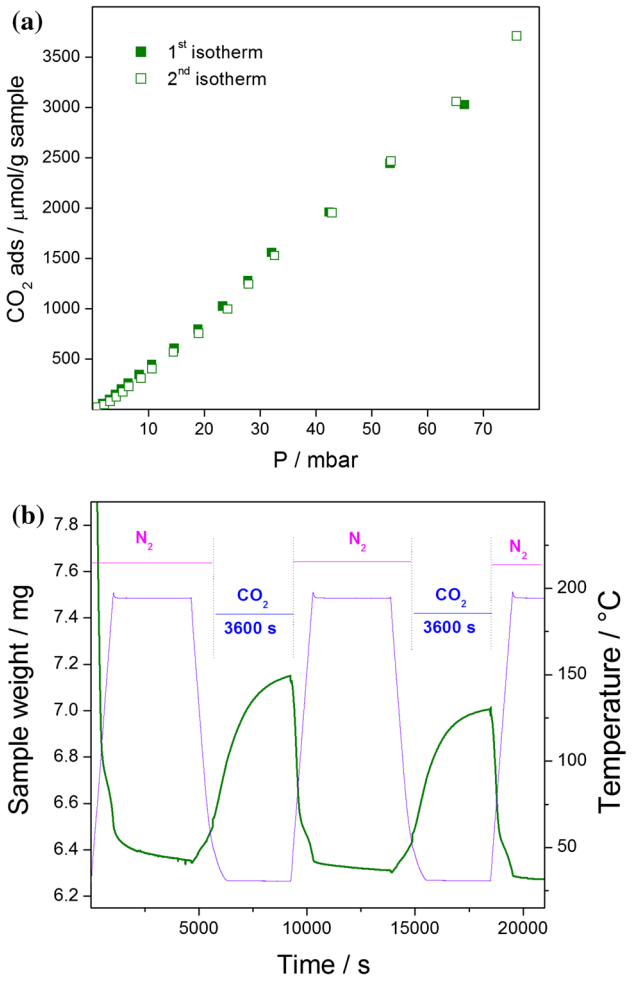

Figure 8 Interaction between UiO-66 nanocrystals and CO_2: **a** CO_2 isotherm at low pressures and 298 K. The adsorption cycle was repeated after evacuation in UHV at 200 °C for 4 h; **b** CO_2 uptake in dynamic conditions with CO_2 flow in a TGA instrument.

pressure, considering that the gas storage is one of the most outstanding applications of this type of materials (Fig. 8a). The test allows verifying that the alternative UiO-66 nanocrystals have a good capacity of interaction with CO_2 at these relatively low pressures and room temperature (3.9 mmol g^{-1}). This CO_2 adsorption capacity is above some reported values for this MOF at similar relative pressure and temperature conditions [3, 25, 37, 38] and could be due to defects in the UiO-66 framework generated by missing linkers. The structural defects lead to greatly increase the porosity and can strongly affect its gas adsorption behavior [37, 38]. However, the amount of CO_2 retained in this MOF can be increased at lower temperatures and higher pressures [4, 23], which can also be concluded from the continuous increase in the

adsorption profile (Fig. 8a). Afterward, the same test was repeated after evacuating the sample in UHV at 200 °C for 4 h and a similar isotherm profile can be observed (Fig. 8a), indicating that the UiO-66 nanocrystals maintain their physicochemical qualities and their ability to act reversibly in the adsorption–desorption process of this probe molecule. Then, another aliquot of the same sample was evaluated in conditions closer to those of real application, analyzing its behavior against CO_2 uptake with pulses under dynamic conditions. It can be seen (Fig. 8b) that the UiO-66 obtained under the modified protocol has a CO_2 capture capacity that reaches values near saturation after 60 min of contact (2.8 mmol g^{-1}). When sweeping with inert gas, there is a reversibility of the process as the sample returns to the same mass value prior to the contact. Repeating this experiment with the same sample, it can be seen that the material exhibits practically the same CO_2 retention capacity and adsorption–desorption profile as at the beginning, indicating that it retains its qualities and has reuse capacity, in agreement with what was observed in low-pressure isotherms.

Conclusions

Nanocrystals of UiO-66 with high specific surface area and yield were obtained using acetone as solvent under mild solvothermal conditions. The synthesis procedure, besides completely replacing the use of DMF as solvent, simplifies the activation process to obtain the free porosity of the MOF. The physicochemical characterizations of the synthesized solids allowed establishing a direct correlation between the efficiency of the synthesis, the crystalline evolution (XRD), the spectral characteristics (FTIR) and its textural qualities. The MOF with better properties was obtained with a Zr: BDC: acetone ratio of 1:1:1622, with a solvothermal treatment at 80 °C for 24 h. The nanocrystals thus obtained have properties comparable to the best ones reported for this MOF obtained in pure DMF [1, 2, 4, 7, 9], with high crystallinity, 150 nm size crystals and surface area of 1299 m^2 g^{-1}. In addition, the UiO-66 showed reversible and high CO_2 uptake capacity at room temperature and low pressure, demonstrating the usefulness of the nanocrystals obtained under optimized conditions in acetone. This simple route of solvothermal synthesis allowed obtaining UiO-66 nanocrystals employing more ecological and economic conditions than those actually reported with conventional solvothermal DMF-based protocols [1–9, 16, 18 20, 33]. Moreover, our protocol could be extended to other Zr-MOFs currently synthesized using DMF such as the case of NU-1000 [31] and NU-1102 [32], since these MOFs are based on the reaction between $ZrCl_4$ and tetracarboxylated ligands. The results bring an advance in the broad field of metal–organic framework synthesis and specifically provide an alternative in the search for new synthetic approaches for this Zr-MOF that has emerged as one of the MOFs with higher application potential in several processes.

Acknowledgements

The authors thank to Consejo Nacional de Investigaciones Científicas y Técnicas (CONICET) from Argentina and also to Prof. José Fernandez for his kind collaboration in the SEM–EDS analyses. This study was funded by Agencia Nacional de Promoción Científica y Tecnológica (ANPCyT) of Argentina (PICT No. 1299), and Universidad Nacional del Litoral, Argentina (CAI + D No. 0486).

Compliance with ethical standards

Conflict of interest The authors declare that they have no conflict of interest.

Electronic supplementary material: The online version of this article (doi:10.1007/s10853-017-1658-5) contains supplementary material, which is available to authorized users.

References

[1] Cavka JH, Jakobsen S, Olsbye U, Guillou N, Lamberti C, Bordiga S, Lillerud KP (2008) A new zirconium inorganic building brick forming metal organic frameworks with exceptional stability. J Am Chem Soc 130:13850–13851

[2] Chavan S, Vitillo JG, Gianolio D, Zavorotynska O, Civalleri B, Jakobsen S, Nilsen MH, Valenzano L, Lamberti C, Lillerud KP, Bordiga S (2012) H_2 storage in isostructural UiO-67 and UiO-66 MOF. Phys Chem Chem Phys 14:1614–1626

[3] Wiersum AD, Soubeyrand-Lenoir E, Yang Q, Moulin B, Guillerm V, Yahia MB, Bourrelly S, Vimont A, Miller S,

Vagner C, Daturi M, Clet G, Serre C, Maurin G, Llewellyn PL (2011) An evaluation of UiO-66 for gas-based applications. Chem Asian J 6:3270–3280

[4] Abid HR, Tian H, Ang H, Tade MO, Buckley CE, Wang S (2012) Nanosize Zr-metal organic framework (UiO-66) for hydrogen and carbon dioxide storage. Chem Eng J 187:415–420

[5] Bozbiyik B, Duerinck T, Lannoeye J, De Vos D, Baron G, Denayer J (2014) Adsorption and separation of *n*-hexane and cyclohexane on the UiO-66 metal–organic framework. Microporous Mesoporous Mater 183:143–149

[6] Zhu X, Gu J, Wang Y, Li B, Li Y, Zhao W, Shi J (2014) Inherent anchorages in UiO-66 nanoparticles for efficient capture of alendronate and its mediated release. Chem Commun 50:8779–8782

[7] Lu Z, Wu M, Wu S, Yang S, Li Y, Liu X, Zheng L, Cao Q, Ding Z (2016) Modulating optical properties of AIE fluophor confined within UiO-66′s nanochannels for chemical sensing. Nanoscale 40:17489–17495

[8] Timofeevaa M, Panchenko V, Won Jun J, Hasan Z, Matrosova M, Hwa Jhung S (2014) Effects of linker substitution on catalytic properties of porous zirconium terephthalate UiO-66 in acetalization of benzaldehyde with methanol. Appl Catal A Gen 471:91–97

[9] Kim S-N, Lee Y-R, Hong S-H, Jang M-S, Ahn W-S (2015) Pilot-scale synthesis of a zirconium-benzenedicarboxylate UiO-66 for CO_2 adsorption and catalysis. Catal Today 245:54–60

[10] Gökpinar S, Diment T, Janiak C (2017) Environmentally benign dry-gel conversions of Zr-based UiO metal–organic frameworks with high yield and possibility of solvent re-use. Dalton Trans 46:9895–9900

[11] Zou C, Vagin S, Kronast A, Rieger B (2016) Template mediated and solvent-free route to a variety of UiO-66 metal–organic frameworks. RSC Adv 6:102968–102971

[12] Seoane B, Zamaro J, Téllez C, Coronas J (2012) Sonocrystallization of zeolitic imidazolate frameworks (ZIF-7, ZIF-8, ZIF-11 and ZIF-20). Cryst Eng Comm 14:3103–3107

[13] Li Y, Liu Y, Gao W, Zhang L, Liu W, Lu J, Wang Z, Deng Y-J (2014) Microwave-assisted synthesis of UIO-66 and its adsorption performance towards dyes. Cryst Eng Comm 16:7037–7042

[14] Faustini M, Kim J, Jeong G-Y, Kim J, Moon H, Ahn W-S, Kim D-P (2013) Microfluidic approach toward continuous and ultra-fast synthesis of metal–organic framework crystals and hetero-structures in confined microdroplets. J Am Chem Soc 135:14619–14626

[15] Bai Y, Dou Y, Xie L, Rutledge W, Li J, Zhou H (2016) Zr-based metal–organic frameworks: design, synthesis, structure, and applications. Chem Soc Rev 45:2327–2367

[16] Ragon F, Horcajada P, Chevreau H, Hwang YK, Lee U-H, Miller SR, Devic T, Chang J-S, Serre C (2014) In situ energy-dispersive X-ray diffraction for the synthesis optimization and scale-up of the porous zirconium terephthalate UiO-66. Inorg Chem 53:2491–2500

[17] Schaate A, Roy P, Godt A, Lippke J, Waltz F, Wiebcke M, Behrens P (2011) Modulated synthesis of Zr-based metal–organic frameworks: from nano to single crystals. Chem Eur J 17:6643–6651

[18] Katz MJ, Brown ZJ, Colón YJ, Siu PW, Scheidt KA, Snurr RQ, Hupp JT, Farha OK (2013) A facile synthesis of UiO-66, UiO-67 and their derivatives. Chem Commun 49:9449–9451

[19] Vermoortele F, Bueken B, Le Bars G, Van de Voorde B, Vandichel M, Houthoofd K, Vimont A, Daturi M, Waroquier M, Van Speybroeck V, Kirschhock C, De Vos DE (2013) Synthesis modulation as a tool to increase the catalytic activity of metal–organic frameworks: the unique case of UiO-66(Zr). J Am Chem Soc 135:11465–11468

[20] Ren J, Langmi HW, North BC, Mathe M, Bessarabov D (2014) Modulated synthesis of zirconium-metal organic framework (Zr-MOF) for hydrogen storage applications. Int J Hydrogen Energy 39:890–895

[21] Han Y, Liu M, Li K, Zuo Y, Wei Y, Xu S, Zhang G, Song C, Zhang Z, Guo X (2015) Facile synthesis of morphology and size-controlled zirconium metal–organic framework UiO-66: the role of hydrofluoric acid in crystallization. Cryst Eng Comm 17:6434–6440

[22] Abid HR, Pham GH, Ang H-M, Tade MO, Wang S (2012) Adsorption of CH_4 and CO_2 on Zr-metal organic frameworks. J Coll Interface Sci 366:120–124

[23] Hu Z, Castano I, Wang S, Wang Y, Peng Y, Qian Y, Chi C, Wang X, Zhao D (2016) Modulator effects on the water-based synthesis of Zr/Hf metal–organic frameworks: quantitative relationship studies between modulator, synthetic condition, and performance. Cryst Growth Des 16:2295–2301

[24] Zhao Q, Yuan W, Liang J, Li J (2013) Synthesis and hydrogen storage studies of metal–organic framework UiO-66. Int J Hydrogen Energy 38:13104–13109

[25] Hu Z, Peng Y, Kang Z, Qian Y, Zhao D (2015) A modulated hydrothermal (MHT) approach for the facile synthesis of UiO-66-type MOFs. Inorg Chem 54:4862–4868

[26] Redlich C, Beckett WS, Sparer J, Barwick KW, Riely CA, Miller H, Sigal SL, Shalat SL, Cullen MR (1988) Liver disease associated with occupational exposure to the solvent dimethylformamide. Ann Intern Med 108:680–686

[27] Dong X, Huang K, Liu S, Ren R, Jin W, Lin YS (2012) Synthesis of zeolitic imidazolate framework-78 molecular-

sieve membrane: defect formation and elimination. J Mater Chem 22:19222–19227

[28] Kandiah M, Nilsen MH, Usseglio S, Jakobsen S, Olsbye U, Tilset M, Larabi C, Quadrelli EA, Bonino F, Lillerud KP (2010) Synthesis and stability of tagged UiO-66 Zr-MOFs. Chem Mater 22:6632–6640

[29] US Environmental Protection Agency (1999) SIDS Initial Assessment Report: Acetone. Report for the 9th SIAM. France

[30] Gales L, Mendes A, Costa C (2000) Hysteresis in the cyclic adsorption of acetone, ethanol and ethyl acetate on activated carbon. Carbon 38:1083–1088

[31] Mondloch JE, Bury W, Fairen-Jimenez D, Kwon S, DeMarco EJ, Weston MH, Sarjeant AA, Nguyen ST, Stair PC, Snurr RQ, Farha OK, Hupp JT (2013) Vapor-phase metalation by atomic layer deposition in a metal–organic framework. J Am Chem Soc 135:10294–10297

[32] Wang TC, Bury W, Gómez-Gualdron DA, Vermeulen NA, Mondloch JE, Deria P, Zhang K, Moghadam PZ, Sarjeant AA, Snurr RQ, Stoddart JF, Hupp JT, Farha OK (2015) Ultrahigh surface area zirconium MOFs and insights into the applicability of the BET theory. J Am Chem Soc 137:3585–3591

[33] Valenzano L, Civalleri B, Chavan S, Bordiga S, Nilsen MH, Jakobsen S, Lillerud KP, Lamberti C (2011) Disclosing the complex structure of UiO-66 metal organic framework: a synergic combination of experiment and theory. Chem Mater 23:1700–1718

[34] Li C-P, Du M (2011) Role of solvents in coordination supramolecular systems. Chem Commun 47:5958–5972

[35] Bustamante E, Fernández J, Zamaro J (2014) Influence of the solvent in the synthesis of zeolitic imidazolate framework-8 (ZIF-8) nanocrystals at room temperature. J Coll Interface Sci 424:37–43

[36] Thommes M, Kaneko K, Neimark AV, Olivier JP, Rodriguez-Reinoso F, Rouquerol J, Sing KSW (2015) Physisorption of gases, with special reference to the evaluation of surface area and pore size distribution (IUPAC Technical Report). Pure Appl Chem 87:1051–1069

[37] Wu H, Chua YS, Krungleviciute V, Tyagi M, Chen P, Yildirim T, Zhou W (2013) Unusual and highly tunable missing-linker defects in zirconium metal–organic framework UiO-66 and their important effects on gas adsorption. J Am Chem Soc 135:10525–10532

[38] Ghosh P, Colón YJ, Snurr RQ (2014) Water adsorption in UiO-66: the importance of defects. Chem Commun 50:11329–11331